NANO LETTERS

pubs.acs.org/NanoLett

Time-Resolved Three-Dimensional Molecular Tracking in Live Cells

Nathan P. Wells,[†,§] Guillaume A. Lessard,[†,||] Peter M. Goodwin,[†] Mary E. Phipps,[†] Patrick J. Cutler,[‡] Diane S. Lidke,[‡] Bridget S. Wilson,[‡] and James H. Werner*[,†]

[†]Center for Integrated Nanotechnologies, Los Alamos National Laboratory, Los Alamos, New Mexico 87545, United States, and [‡]Department of Pathology, University of New Mexico Health Sciences Center, Albuquerque, New Mexico 87131, United States

ABSTRACT We report a method for tracking individual quantum dot (QD) labeled proteins inside of live cells that uses four overlapping confocal volume elements and active feedback once every 5 ms to follow three-dimensional molecular motion. This method has substantial advantages over three-dimensional molecular tracking methods based upon charge-coupled device cameras, including increased *Z*-tracking range (10 μm demonstrated here), substantially lower excitation powers (15 μW used here), and the ability to perform time-resolved spectroscopy (such as fluorescence lifetime measurements or fluorescence correlation spectroscopy) on the molecules being tracked. In particular, we show for the first time fluorescence photon antibunching of individual QD labeled proteins in live cells and demonstrate the ability to track individual dye-labeled nucleotides (Cy5-dUTP) at biologically relevant transport rates. To demonstrate the power of these methods for exploring the spatiotemporal dynamics of live cells, we follow individual QD-labeled IgE-FcεRI receptors both on and inside rat mast cells. Trajectories of receptors on the plasma membrane reveal three-dimensional, nanoscale features of the cell surface topology. During later stages of the signal transduction cascade, clusters of QD labeled IgE-FcεRI were captured in the act of ligand-mediated endocytosis and tracked during rapid (~950 nm/s) vesicular transit through the cell.

KEYWORDS Quantum dot, single molecule, fluorescence, tracking, microscopy, cell

The direct observation of individual biological molecules in motion can transform our view of important biophysical and cellular processes.[1] For example, single molecule tracking has shed significant light on cellular membrane dynamics,[2−4] motor protein kinetics,[5,6] and gene regulation.[7] Advantages of a single molecule approach include the ability to observe dynamic, stochastic behavior (such as compartmentalized diffusion[2,4]) that would be masked in ensemble measurements and the ability for localization of molecules with a precision well below the diffraction limit of light.[5,6] To date the field has primarily relied on wide-field imaging with a charge-coupled device (CCD) camera, a method that generally captures spatiotemporal dynamics in only two dimensions.

While following the motion of individual molecules in two dimensions is a proven and powerful method to explore biomolecular function, most aspects of life, including protein and RNA trafficking, inherently involve motion throughout three spatial dimensions. Unfortunately, tracking single molecules moving through three dimensions is a difficult, and until recently,[8−15] unsolved technical problem. Many of the newly developed approaches to three-dimensional (3D) molecular tracking use CCD cameras, either encoding *Z* information in their point-spread function[8,10] or follow the *Z* position with multiple cameras or image planes.[9,14] While these camera-based techniques can capture 3D molecular motion, they are generally limited in their Z-tracking range in cells to approximately ± 1 μm from a fixed focal plane,[8,10,14,16] due to the shallow depth of field of high numerical aperture microscope objectives needed for single molecule work. We point out the obvious: many cells are substantially thicker than 2 μm and different methods and techniques are required to follow single molecules throughout entire three-dimensional cell volumes. In addition to its quite limiting *Z*-tracking range, CCD-based tracking approaches are also bounded in temporal resolution by the CCD frame rate (~1 ms for fast EM-CCDs) and must illuminate an entire cell slice at relatively large excitation intensities (~40 W/cm^2).

In contrast to 3D molecular tracking based upon CCD cameras, 3D molecular tracking with confocal feedback[11−13,15,17] offers substantial advantages. First, the *Z*-tracking range is not limited by the depth of field of the objective (~1−2 μm), but rather is limited by the travel of the stage (10 μm) and ultimately limited by the working distance of the objective (~200 μm for the water immersion objective used here). This increase in *Z*-tracking range enables tracking biomolecular motion throughout the entire volume of many mammalian cells. Second, the temporal resolution is limited by the instrument response of a single element detector (~400 ps for single photon counting avalanche photodioes) and can thus potentially follow fast, dynamic motion on time scales

* To whom correspondence should be addressed. E-mail: jwerner@lanl.gov.

[§] Current Address: Aerospace Corporation, El Segundo, California 90245.

[||] Current Address: Covidien, Boulder, Colorado 80301.

Received for review: 09/14/2010
Published on Web: 00/00/0000

DOI: 10.1021/nl103247v | *Nano Lett.* **XXXX,** *xxx,* 000–000

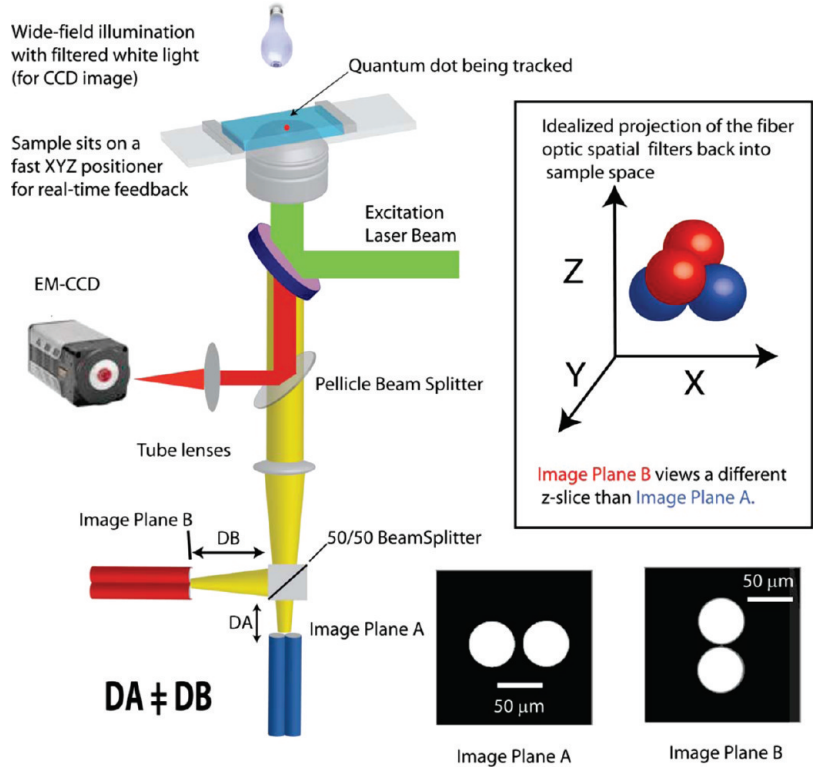

FIGURE 1. Schematic of the 3D tracking apparatus. Four fiber optics serve as spatial filters to examine four nearly diffraction limited spots in the sample simultaneously. Because of the spacing and arrangement of the fibers, these four spots form a 3D tetrahedron in the sample space. While tracking, active feedback of a *XYZ* piezo stage is used to keep counts on all four detectors equal and as large as possible. A small fraction (~8%) of the emission from the molecule being tracked is sent to an EM-CCD camera, which enables contextual information for the position of the molecule in the cell during 3D tracking.

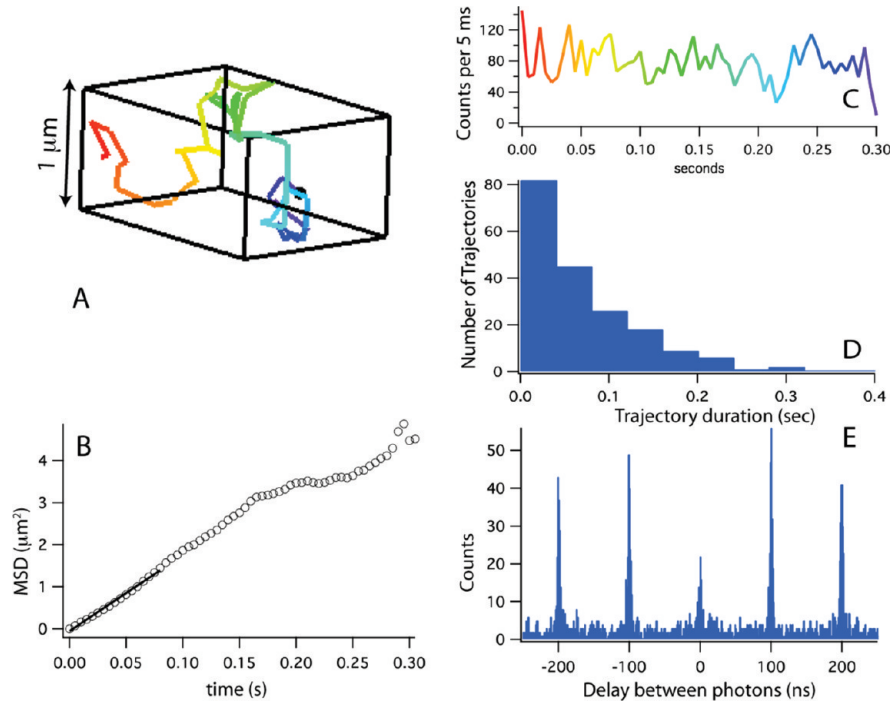

FIGURE 2. (A) A 3D trajectory for a single Cy5-dUTP tracked in a 90:10 glycerol/water mixture. (B) An analysis of the MSD for this ~0.3 s long trajectory. A linear fit (solid line) to the first one-fourth of the trajectory returns a diffusion coefficient of ~3 μm^2/sec. (C) Counts obtained during this 3D track. (D) A histogram of track durations shows approximately 25% of the tracks last longer than 0.1 s. (E) A photon-pair correlation histogram obtained by summing the pair correlations obtained from 50 tracks that lasted longer than 0.1 s. The observed photon antibunching behavior demonstrates these trajectories are from individual Cy5-dUTP molecules.

DOI: 10.1021/nl103247v | *Nano Lett.* **XXXX,** *xxx,* 000–000

orders of magnitude faster than CCDs[18] or perform time-resolved spectroscopy on the molecules being followed.[11,15] Third, as confocal excitation employs a tightly focused laser beam, whole-cell oxidative photodamage is substantially less than it is for wide-field excitation.

Our previous investigations using 3D tracking via four overlapping confocal volume elements demonstrated one can follow individual quantum dots in three dimensions at biologically relevant transport rates[13] and in high background environments.[15] Here we show the same 3D tracking method can be used to follow protein traffic in live cells. In brief, our method uses four fiber optics as spatial filters (see Figure 1) to simultaneously monitor four, near diffraction limited, points in the sample. Because of the arrangement and spacing of the fiber optics with respect to the tube lens of the microscope, the aggregate optical probe volume forms a three-dimensional tetrahedron in the sample space. We note that even though the fiber optics have a small (~10 μm) gap between them (Figure 1), the four detection volumes in the sample space overlap to a large extent (Figure S1 of the Supporting Information). In particular, when the fluorescence image of a quantum dot is placed between two fibers, the sum of the counts for both detectors in a given image plane is only ~10% less than the sum of the counts obtained when the quantum dot image is exactly centered on one of the fibers (Supporting Information Figure S1). When a single fluorescent molecule is present in the probe volume, active feedback of a fast *XYZ* piezo stage is used to keep the counts on all four photon detectors equal and as large as possible with the stage position adjusted once every 5 ms.[15] The three-dimensional localization accuracy for a single quantum dot in 5 ms is ~50 nm in *X*,*Y* and ~80 nm in *Z*, with the localization accuracy improving approximately with the square root of the integration period (Supporting Information Figure S2). We note our approach to 3D molecular tracking is in many ways reminiscent of Berg's pioneering methods of following individual bacteria during chemotaxis,[19,20] with the following exceptions: we employ four detectors (rather than six) for 3D positional sensitivity, we use pulsed excitation and time-correlated single photon counting to record the arrival time of every photon detected with ~400 ps accuracy, and we can follow small, dim objects such as single quantum dots[13,15] or single organic dyes (see Figure 2).

As a model system for following protein traffic in live cells, we take advantage of monovalent QD-IgE^{DNP} probes, previously shown to bind intact FcεRI on the surface of the

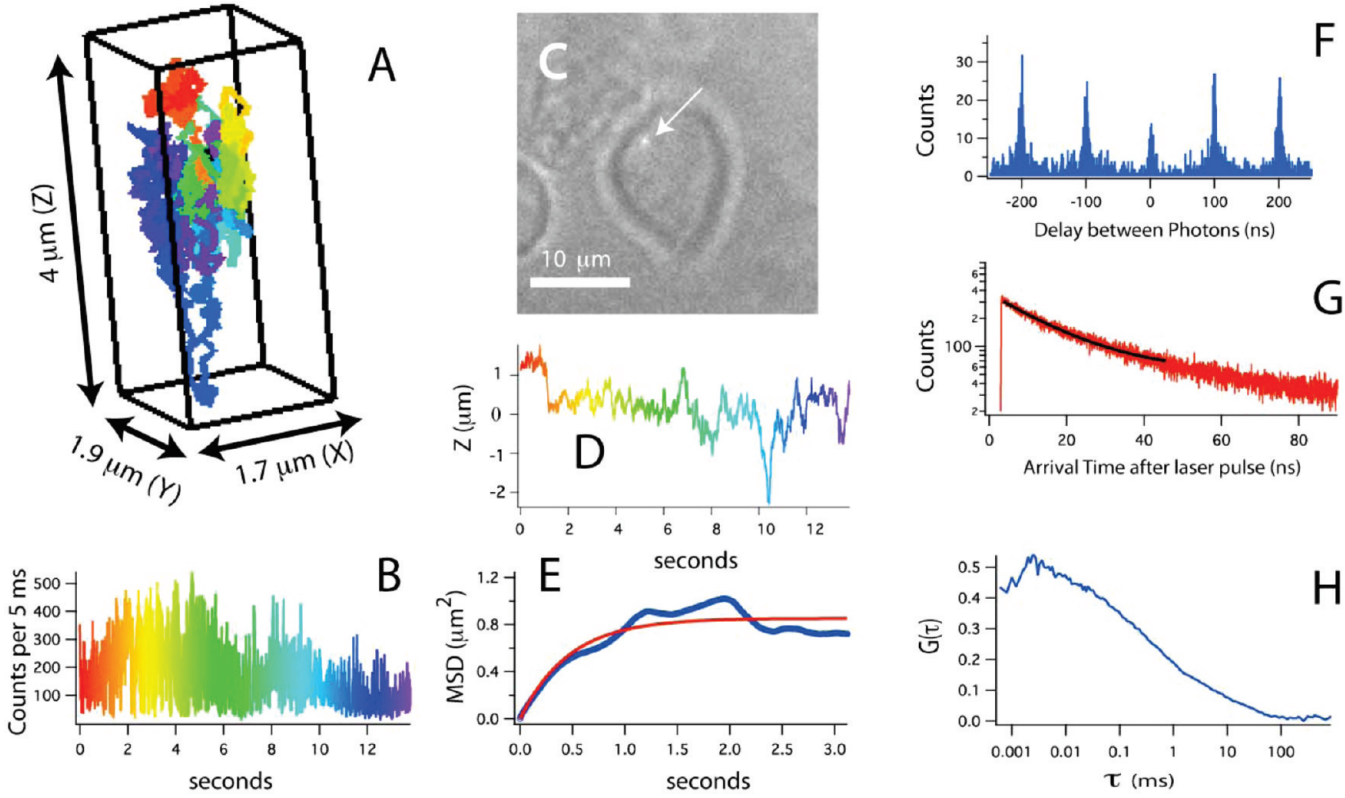

FIGURE 3. (A) Three-dimensional trajectory of a single QD labeled IgE-FcεRI on an unstimulated mast cell at 37 °C. A rainbow color scheme is used to denote the passage of time. (B) The counts used for 3D tracking and feedback. (C) A CCD image showing the receptor location relative to the mast cell (arrow points to QD). (D) The *Z*-position of this receptor, showing over 4 μm of *Z*-motion that would be missed in CCD-based tracking methods. (E) The mean-squared displacement (blue) and fit (red). The motion is highly compartmentalized and is fit using eq 3 of the Supporting Information. (F) A photon pair correlation measurement derived from this ~14 s long trajectory that shows fluorescence photon antibunching. (G) A histogram of photon arrival times with respect to the excitation laser pulse (red) and exponential fit (black), which yields a 16 ns fluorescence lifetime. (H) An autocorrelation analysis of photon detection rate obtained during this trajectory. The decay in the correlation curve is dominated by quantum dot blinking dynamics.

DOI: 10.1021/nl103247v | *Nano Lett.* **XXXX,** *xxx,* 000–000

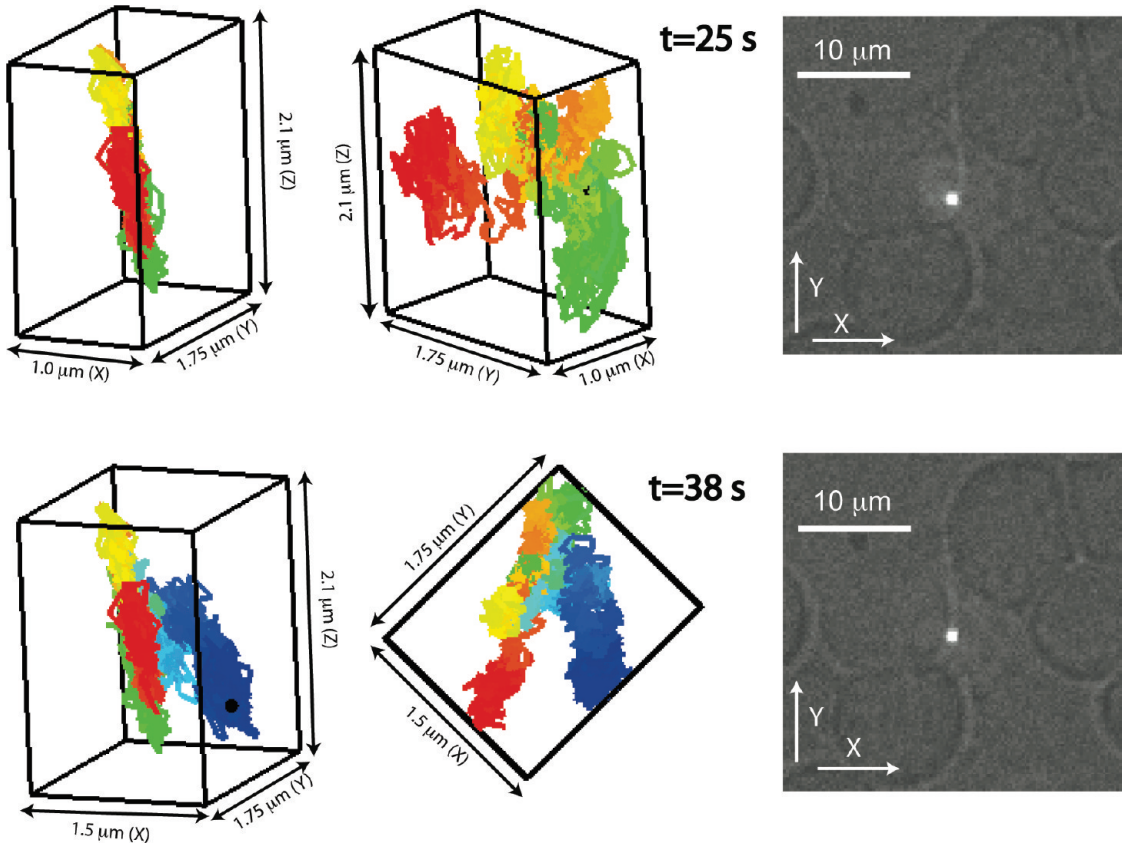

FIGURE 4. (Top) Two representations of a 3D trajectory QD-IgE-FcεRI taken 25 s into the trajectory and CCD image of the receptor position with respect to the cell. At this time, the trajectory is primarily 2D and is clearly on the side of the cell. (Bottom) Later in the trajectory, this QD-IgE-FcεRI ventures perpendicularly outward from the main cell body.

RBL-2H3 rat tumor mast cell line without perturbing the activation state of the receptor.[4] Cross-linking of multiple QD-IgE-FcεRI complexes with polyvalent ligand (DNP[23]-BSA) leads to receptor activation, inducing a complex tyrosine kinase cascade and release of histamine and other inflammatory mediators.[21] FcεRI cross-linking also induces marked changes in cell morphology, including extensive membrane ruffling[22] and receptor internalization.[23]

Figure 3 and Supporting Information movie SM3 show a 3D trajectory of a single QD-labeled IgE-FcεRI complex on the side of an unstimulated mast cell at 37 °C. This trajectory shows we can follow motion over several micrometers in the *Z*-dimension (Figure 3A,D) and also highlights the time-resolved spectroscopies that can be performed while tracking (Figure 3F−H). During the ∼14 s observation period, the QD-IgE-FcεRI motion follows a complex 3D topology on the side of the mast cell that includes motion over 4 μm in the *Z*-direction (Figure 3A,D). The mean-squared displacement (MSD; Figure 3E, blue) for this trajectory shows highly corralled diffusion (with a corral size of ∼1.6 μm) with fits to the early portion of the MSD revealing an intercorral (or instantaneous) diffusion rate of 0.21 μm^2/sec, which is slightly faster than previous measurements of IgE-FcεRI diffusion on the basal membrane surface.[4]

In addition to recording the entire XYZ trajectory for this single molecule, the arrival time of every photon is recorded with ∼400 ps time resolution. Recording the arrival times of individual photons opens the door to time-resolved analysis methods impossible with conventional CCD cameras. Three methods of analyzing this data are shown in Figure 3F−H. Figure 3F shows a histogram of the delay times between adjacent detected photons (a pair correlation measurement), showing fluorescence photon antibunching[24,25] from a single quantum dot undergoing motion on a live cell (the central peak is nonzero due to the background cellular autofluorescence[15,26]). The fact the photons are antibunched in time (i.e., we infrequently detect two photons simultaneously) is a rigorous demonstration that this track is of a single quantum system.[24,25] Another means of analyzing the raw photon data is to construct a histogram of photon arrival times with respect to the laser pulse (Figure 3G), which measures the fluorescence lifetime of the QD. Here we show the histogram for the entire trajectory, but we have previously shown this information can also be obtained as a function of time/molecule position.[15] In Figure 3H, fluorescence correlation spectroscopy (FCS)[27] is used to analyze the fluctuations in emission intensity observed during the trajectory with the correlation decay for this trajectory being

DOI: 10.1021/nl103247v | *Nano Lett.* **XXXX,** *xxx,* 000–000

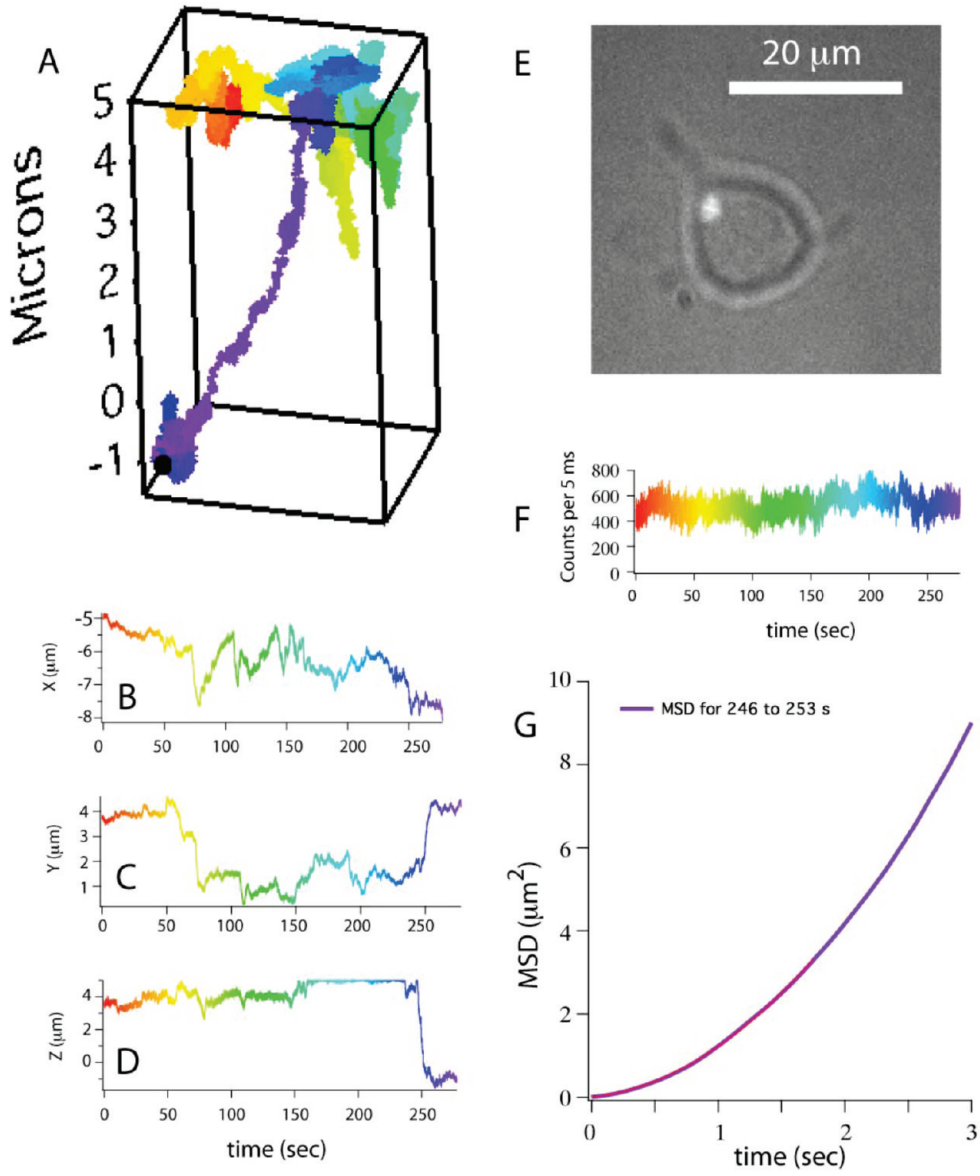

FIGURE 5. (A) A 3D trajectory obtained from a single signaling patch of approximately five quantum dot-labeled IgE-FcεRI. A rainbow color scheme is used to denote the passage of time. (B−D) The *X*, *Y*, and *Z* position of this cluster. Between ∼160−235 s, the cluster is near the maximum travel of the piezo stage in the +*Z* dimension (+5 μm). While the cluster is at the maximum of our positive Z travel, it is not lost, as the counts do not significantly drop, the image of the cluster remains in focus (Supporting Information Movie M5), and we often give stage commands that move in the minus *Z* direction. (E) The image of this cell obtained by the CCD camera near the beginning of the track. (F) The counts used for feedback and tracking. (G) The MSD for 246−253 s period (purple) and fit (red). The MSD is parabolic, indicative of directed motion. A fit to the MSD using eq 2 of the Supporting Information yields a transport velocity of 950 nm/sec for the steep plunge occurring between 246 and 253 s.

dominated by QD blinking.[28] FCS is a powerful analysis method to observe biomolecular conformational fluctuations[29,30] or to probe dynamics in live cells.[31,32] However, in general, observation times for most FCS measurements are limited to the transit of the molecule through the optical probe volume (∼10 ms or less). Here, we demonstrate that FCS can be performed on the same molecule in a live cell for an extended time period even while this molecule is moving at biological transport rates.

In addition to the temporal resolution afforded by confocal 3D tracking, the path of single QD-IgE-FcεRI can map out complex 3D topologies on cell surfaces,[33] as demonstrated in Figure 4. During the first 25 s, the motion of this receptor is essentially two-dimensional with this 2D surface (the cell membrane) being nearly perpendicular to the *XY* plane. However, this receptor then ventures perpendicular to cell membrane it has previously been confined to, mapping out a complex 3D nanotopology (most likely a cellular filopodia).

DOI: 10.1021/nl103247v | *Nano Lett.* **XXXX,** *xxx,* 000−000

Another example of 3D tracking mapping out 3D membrane topology is given by Supporting Information Figure S6 and Movie SM6, which show a the 3D trajectory for a single QD-IgE-FcεRI on a highly curved region of the plasma membrane.

While our ability to follow individual quantum dot labeled IgE-FcεRI receptors is usually limited by long-lived (>10 ms) dark states (i.e., QD blinking[15,28]), aggregated, cross-linked clusters of multiple IgE-FcεRI receptors (each labeled with a QD) can be followed for very long time periods (several minutes). This is shown in Figure 5 and Supporting Information Movie SM5, where a cluster of ~5 QD-IgE-FcεRI receptors travels on the apical cell membrane for several minutes after the addition of antigen. Changes in the Z position during this phase are consistent with travels across a ruffled landscape[22] created by dynamic rearrangement of the underlying actin cytoskeleton. At ~250 s into observation, the receptor complex is taken up into an endocytic vesicle, plunging nearly 7 μm into the cell interior and reaching an average velocity of 950 nm/sec during this transport event, consistent with previous measures of endocytic transport rates.[34] Additional examples of large-scale *Z*-directional motion in QD-IgE-FcεRI complexes, observed in antigen-stimulated RBL-2H3 cells, are found in the Supporting Information (Figures S7, S8, and S9 and Movies SM7, SM8, and SM9).

In summary, we have demonstrated a confocal tracking method capable of following individual quantum dot-labeled signaling molecules, in three dimensions, on and inside living cells. Trajectories can be measured for minutes and can extend up to 10 μm in all spatial dimensions, enabling tracking throughout the entire volume of many mammalian cells. In addition to the substantial kinetic data obtained from these three-dimensional trajectories, individual photon arrival times are recorded with ~400 ps accuracy, enabling a number of time-resolved analysis methods impossible with camera-based tracking methods.

Acknowledgment. This work is supported by the National Institutes of Health (No. R21AI07707 to J.H.W., AI051575 to B.S.W., and P50GM065794) and was performed at the Center for Integrated Nanotechnologies, a U.S. Department of Energy, Office of Basic Energy Sciences user facility. Los Alamos National Laboratory is operated by Los Alamos National Security, LLC, for the National Nuclear Security Administration of the U.S. Department of Energy under contract DE- AC52-06NA25396.

Supporting Information Available. Materials and Methods and a list of equations used for fitting and data analysis are included. Supporting figures include 1D slices and 2D contour plots of our combined excitation/collection efficiency (S1) and an experimental measure of our tracking accuracy as a function of integration time (S2), and selected 3D trajectories of QD-IgE-FcεRI on and inside antigen-stimulated (Figures S7–S9) and unstimulated (Figure S6) mast cells. QuickTime movies, which show how the 3D trajectories of QD-IgE-FcεRI evolve with time, are available for all trajectories shown in the main text and in the Supporting Information. This material is available free of charge via the Internet at http://pubs.acs.org.

REFERENCES AND NOTES

(1) Pinaud, F.; Clarke, S.; Sittner, A.; Dahan, M. *Nat. Methods* **2010**, *7* (4), 275–285.
(2) Fujiwara, T.; Ritchie, K.; Murakoshi, H.; Jacobson, K.; Kusumi, A. *J. Cell Biol.* **2002**, *157* (6), 1071–1081.
(3) Dahan, M.; Levi, S.; Luccardini, C.; Rostaing, P.; Riveau, B.; Triller, A. *Science* **2003**, *302* (5644), 442–445.
(4) Andrews, N. L.; Lidke, K. A.; Pfeiffer, J. R.; Burns, A. R.; Wilson, B. S.; Oliver, J. M.; Lidke, D. S. *Nat. Cell Biol.* **2008**, *10* (8), 955–963.
(5) Gelles, J.; Schnapp, B. J.; Sheetz, M. P. *Nature* **1988**, *331* (6155), 450–453.
(6) Yildiz, A.; Forkey, J. N.; McKinney, S. A.; Ha, T.; Goldman, Y. E.; Selvin, P. R. *Science* **2003**, *300* (5628), 2061–2065.
(7) Elf, J.; Li, G. W.; Xie, X. S. *Science* **2007**, *316* (5828), 1191–1194.
(8) Holtzer, L.; Meckel, T.; Schmidt, T. *Appl. Phys. Lett.* **2007**, *90*, 053902.
(9) Toprak, E.; Balci, H.; Blehm, B. H.; Selvin, P. R. *Nano Lett.* **2007**, *7* (7), 2043–2045.
(10) Thompson, M. A.; Lew, M. D.; Badieirostami, M.; Moerner, W. E. *Nano Lett.* **2010**, *10* (1), 211–218.
(11) McHale, K.; Berglund, A. J.; Mabuchi, H. *Nano Lett.* **2007**, *7* (11), 3535–3539.
(12) Cang, H.; Xu, C. S.; Montiel, D.; Yang, H. *Opt. Lett.* **2007**, *32* (18), 2729–2731.
(13) Lessard, G.; Goodwin, P. M.; Werner, J. H. *Appl. Phys. Lett.* **2007**, *91* (22), 2224106.
(14) Ram, S.; Prabhat, P.; Chao, J.; Ward, E. S.; Ober, R. J. *Biophys. J.* **2008**, *95* (12), 6025–6043.
(15) Wells, N. P.; Lessard, G. A.; Werner, J. H. *Anal. Chem.* **2008**, *80* (24), 9830–9834.
(16) Mlodzianoski, M.; Juette, M.; Beane, G.; Bewersdorf, J. *Opt. Express* **2009**, *17* (10), 8264–8277.
(17) Levi, V.; Ruan, Q. Q.; Gratton, E. *Biophys. J.* **2005**, *88* (4), 2919–2928.
(18) Sahl, S.; Leutenegger, M.; Hilbert, M.; Hell, S.; Eggeling, C. *Proc. Natl. Acad. Sci. U.S.A.* **2010**, *107* (15), 6829–6834.
(19) Berg, H. C. *Rev. Sci. Instrum.* **1971**, *42* (6), 868–871.
(20) Berg, H. C.; Brown, D. A. *Nature* **1972**, *239* (5374), 500.
(21) Andrews, N.; Pfeiffer, J.; Martinez, A.; Haaland, D.; Davis, R.; Kawakami, T.; Oliver, J.; Wilson, B.; Lidke, D. *Immunity* **2009**, *31* (3), 469–479.
(22) Pfeiffer, J.; Seagrave, J.; Davis, B.; Deanin, G.; Oliver, J. *J. Cell Biol.* **1985**, *101* (6), 2145.
(23) Barker, S.; Caldwell, K.; Hall, A.; Martinez, A.; Pfeiffer, J.; Oliver, J.; Wilson, B. *Mol. Biol. Cell* **1995**, *6* (9), 1145–1158.
(24) Kimble, H. J.; Dagenais, M.; Mandel, L. *Phys. Rev. Lett.* **1977**, *39* (11), 691–695.
(25) Michler, P.; Imamoglu, A.; Mason, M. D.; Carson, P. J.; Strouse, G. F.; Buratto, S. K. *Nature* **2000**, *406* (6799), 968–970.
(26) Weston, K. D.; Dyck, M.; Tinnefeld, P.; Muller, C.; Herten, D. P.; Sauer, M. *Anal. Chem.* **2002**, *74* (20), 5342–5349.
(27) Magde, D.; Elson, E. L.; Webb, W. W. *Biopolymers* **1974**, *13* (1), 29–61.
(28) Nirmal, M.; Dabbousi, B. O.; Bawendi, M. G.; Macklin, J. J.; Trautman, J. K.; Harris, T. D.; Brus, L. E. *Nature* **1996**, *383* (6603), 802–804.
(29) Werner, J. H.; Joggerst, R.; Dyer, R. B.; Goodwin, P. M. *Proc. Natl. Acad. Sci. U.S.A.* **2006**, *103* (30), 11130–11135.
(30) Bonnet, G.; Krichevsky, O.; Libchaber, A. *Proc. Natl. Acad. Sci. U.S.A.* **1998**, *95* (15), 8602–8606.
(31) Bacia, K.; Kim, S. A.; Schwille, P. *Nat. Methods* **2006**, *3* (2), 83–89.
(32) Eggeling, C.; Ringemann, C.; Medda, R.; Schwarzmann, G.; Sandhoff, K.; Polyakova, S.; Belov, V. N.; Hein, B.; Von Middendorff, C.; Schonle, A.; Hell, S. W. *Nature* **2009**, *457* (7233), 1159–1162.
(33) Wells, N. P.; Lessard, G. A.; Phipps, M. E.; Goodwin, P. M.; Lidke, D. S.; Wilson, B. S.; Werner, J. H. *Proc. SPIE* **2009**, *7185*, 7185-1–7185-13.
(34) Nan, X.; Sims, P.; Chen, P.; Xie, X. *J. Phys. Chem. B* **2005**, *109* (51), 24220–24224.

DOI: 10.1021/nl103247v | *Nano Lett.* **XXXX,** *xxx,* 000–000